Spectrochimica Acta Part A: Molecular and Biomolecular Spectroscopy xxx (xxxx) xxx

Contents lists available at ScienceDirect

Spectrochimica Acta Part A: Molecular and Biomolecular Spectroscopy

journal homepage: www.elsevier.com/locate/saa

Controlled fabrication of gold nanobipyramids/polypyrrole for shell-isolated nanoparticle-enhanced Raman spectroscopy to detect γ-aminobutyric acid

Waleed Ahmed El-Said [a,b,c], Wael Alshitari [c], Jeong-woo Choi [a,*]

[a] Department of Chemical and Biomolecular Engineering, Sogang University, 35, Baekbeom-Ro, Mapo-Gu, Seoul 04107, Republic of Korea
[b] Department of Chemistry, Faculty of Science, Assiut University, Assiut 71516, Egypt
[c] University of Jeddah, College of Science, Department of Chemistry, P.O. 80327, Jeddah 21589, Saudi Arabia

ARTICLE INFO

Article history:
Received 31 July 2019
Received in revised form 27 November 2019
Accepted 1 December 2019
Available online xxxx

Keywords:
γ-Aminobutyric acid
Glutamate
Gold nanobipyramids
Polypyrrole
Shell-isolated nanoparticle-enhanced Raman spectroscopy

ABSTRACT

Shell-isolated nanoparticle-enhanced Raman Spectroscopy (SHINERS) has been a non-destructive, highly sensitive, specific and powerful sensing method. Detection of γ-aminobutyric acid (GABA) and glutamate, main neurotransmitters in the human brain, is important to diagnosis the neurological disorder. The purpose of this study is preparing a simple, rapid and inexpensive fabrication of Au nanobipyramids/polymer core/shell as a SHINERS-based biosensor to detect different neurotransmitters such as GABA and glutamate with high sensitivity and specificity. Au nanobipyramids/polymer core/shell was fabricated by using two steps process. In the first Au nanobipyramids with longitude and latitude axial of about 100 nm and 10 nm, respectively, was prepared based on the chemical reduction of Au ions by using sodium borohydride as a reducing agent. Then a thin layer of polypyrrole was used for decorating the Au nanobipyramids by using direct polymerization in the presence of Au nanobipyramids. The sensor composed Au nanobipyramids with a thin layer of polypyrrole that could measure GABA within a wide range of concentrations in the presence of human serum. And this sensor was used for direct monitoring of GABA and glutamate. The proposed biosensor can be applied to monitor the level of neurotransmitters accurately for the diagnosis of various neurological disorders with optical signal enhancement.

1. Introduction

Raman spectroscopy represented one of the vital nondestructive analytical techniques that possess many advantages including high specificity, quick response and its ability to provide rich information about the target species without needing for sample preparation. Nevertheless, the weak Raman intensity has limited its applications for detecting trace species. Several techniques were applied for improving the intensity of the Raman signals; among these techniques, surface-enhanced Raman scattering (SERS) is the most commonly used Raman enhancement technique [1] that enabling detection at very low concentration levels with high specificity and sensitivity in presence of metal nanoparticles [2]. Several noble metals including silver (Ag), gold (Au) or copper (Cu) nanostructures with different sizes and shapes have been used as high active-SERS agents [3–7]. The chemical nature, dimensions, morphology, and spacing of the nanomaterials play the main influences on the intensity of the SERS signals. Ag at the nanoscale is the first materials used for enhancing the Raman intensity; furthermore, Ag and Au's nanostructures represented the widely used SERS-based agents for the different applications. Although there is notable progress in SERS research, many challenges achieving a repeatable and quantitative SERS signal and fabrication of uniform and stable nanoparticles hindering its development.

Biosensors (optical or electrical biosensors) could be divided into label-based [8] and label-free biosensors [9]. Label-free biosensors are advantages due to their simple cost-effective, speed detection, easier and direct detection properties. Recently, Choi's group have used Au nanostar/ITO for monitoring the neural stem cell differentiation [3] detecting dopamine neurotransmitter [4], β-amyloid peptide [5], and study effects of some chemotherapeutic agents towards different cancer cells [6] based on SERS technique. The PANI/Au nanodots/ITO electrode was used as an electrochemical biosensor for the rapid and simultaneous determination of different purine bases [10]. Also, Au nanodots/ITO was used for investigating the intracellular and extracellular redox states of the neural cells based on Spectroelectrochemical (Raman spectroscopy and linear sweep voltammetry) method detect several targets at a very highly sensitive level [7].

* Corresponding author at: Department of Chemical & Biomolecular Engineering, Sogang University, Seoul, Republic of Korea.
E-mail address: jwchoi@sogang.ac.kr (J. Choi).

https://doi.org/10.1016/j.saa.2019.117890
1386-1425/

γ-Aminobutyric acid (GABA) considered as one of the main inhibitory neurotransmitters [11], while glutamate (Glu) is among the main excitatory neurotransmitters [12] in the central nervous system (CNS). They play vital roles in decreasing neuronal excitability throughout the CNS [13]. Changes in the Glu and GABA levels were accompanied by neurological and psychiatric disorders, for example, epilepsy, schizophrenia, and Alzheimer's disease [14–18].

Therefore, monitoring the changes in the concentrations of the neurotransmitters may offer an additional tool for several studies, including drug design, elucidation of CNS function and dysfunction accompanying different kinds of brain insult, nursing drug efficiency or drug abuse. The detection of very low levels of GABA needs highly selective assays such as high-performance liquid chromatography (HPLC) combined with either fluorescence or electrochemical detection, liquid chromatography/mass spectrometry and liquid chromatography/tandem mass spectrometry were used for detecting GLU and GABA in biological samples [19,20]. However, GABA and Glu themselves are neither fluorescent nor electroactive, so they need derivatization prior to detection [21–24]. Elution and derivatization are time-consuming processes that limited the applications of HPLC uses for analysis of Glu and GABA neurotransmitters [23–25]. Additionally, these methods are very time-consuming, complicated procedures and their accessories are highly cost [26]. Capillary electrophoresis-laser-induced fluorescence was also used for monitoring of GABA neurotransmitter [27]; nonetheless, it also needed a derivatization process that increased the cost and longer time is needed.

SERS have been applied independently for monitoring the neurotransmitters (e.g. GLU, GABA, and norepinephrine) levels [28–31]. The simultaneous measurement of GLU and GABA is vital for correct analysis of neurological disorders, and the potential for evolving novel neuropharmacological agents [32]. However, owing to the similarity in chemical structures of Glu and GABA, there is an overlapping between the Raman bands of GLU and GABA; thus it is needed the uses the signal processing techniques such as the principal component analysis (PCA) technique to differentiate between them. Therefore, there is an urgent need for simple and cost-effective procedures that can provide a precise, simultaneous and fast measuring of GLU and GABA.

Li and his group have reported on fabrication an ultrathin of silica or alumina shell coated Au or Ag NPs and their uses as shell-isolated nanoparticle-enhanced Raman spectroscopy (SHINERS) for enhancing the intensity of the Raman signals [33]. Recently, several SHINERS including polymers, graphene and graphene's derivatives films were fabricated and studied [34–48], this shell could inhibit the nanomaterials agglomeration, improves their stability, preserves the metals NPs isolate them from the direct connection with the probed material and allows the NPs to adapt with different contours of substrates. This shell-isolated could offer strong enhancement of the Raman effect and hence provide highly sensitive and diverse practical applications to numerous materials. However, still, there is an urgent needing for the fabrication of new SHINERS and its biological application.

Here, we have fabricated Au nanobipyramids (Au NbPs) and coated them with a thin layer of polypyrrole as an isolated shell. Then, we have used the isolated shell polypyrrole/Au NbPs as label-free biosensors based on the SERS technique for direct detection of GLU and GABA neurotransmitters dissolved in PBS (pH, 7.4) solution with a detection limit of 1.16 nM, also we have detected GABA neurotransmitter soluble in human serum.

2. Experimental

2.1. Materials

Pyrrole, ammonium persulfate (98%), ascorbic acid, sodium borohydride ($NaBH_4$), hexadecyltrimethylammonium bromide (CTAB, 98%) and $HAuCl_4 \cdot 3H_2O$ were purchased from Sigma-Aldrich. Sodium dodecyl

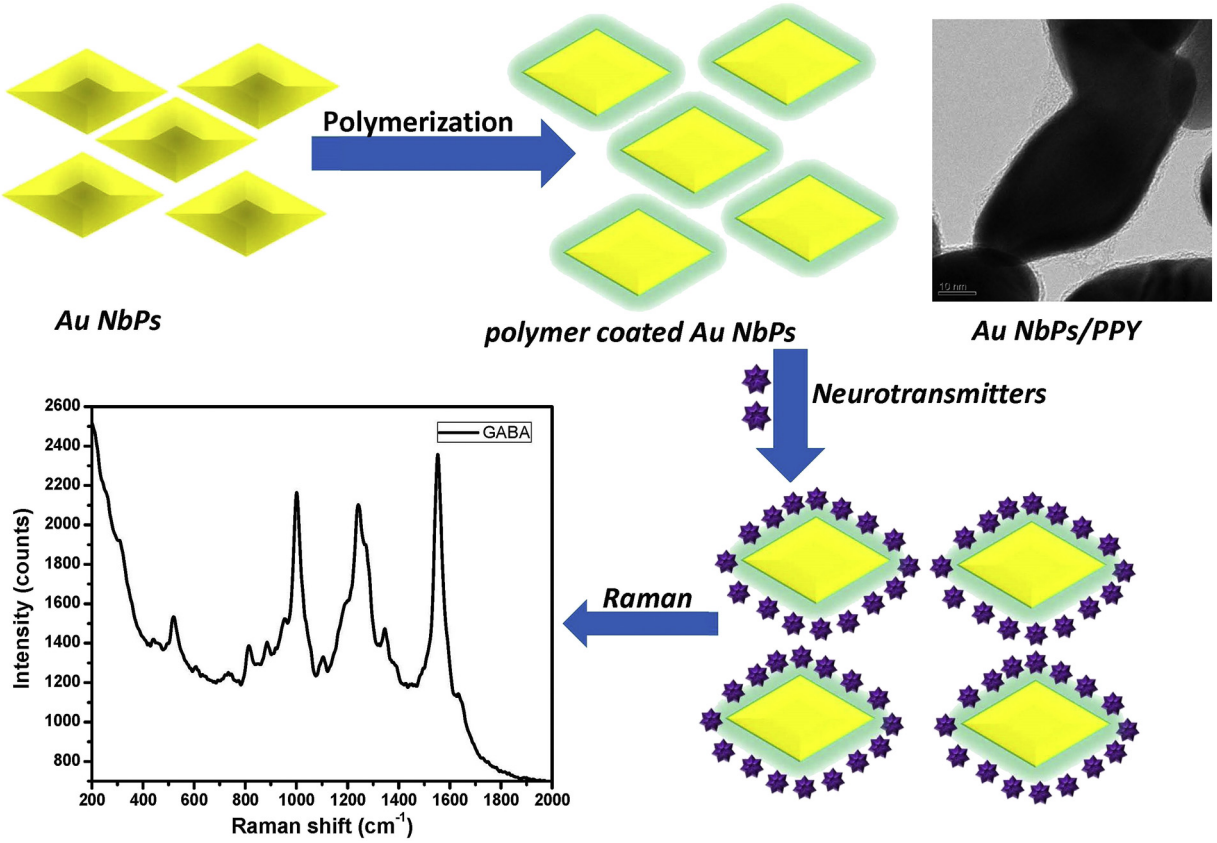

Scheme 1. Schematic diagram of the neurotransmitters biosensor by using Au NbPs/PPy based on surface-enhanced Raman spectroscopy technique

Please cite this article as: W.A. El-Said, W. Alshitari and J. Choi, Controlled fabrication of gold nanobipyramids/polypyrrole for shell-isolated nanoparticle-enhanced R..., Spectrochimica Acta Part A: Molecular and Biomolecular Spectroscopy, https://doi.org/10.1016/j.saa.2019.117890

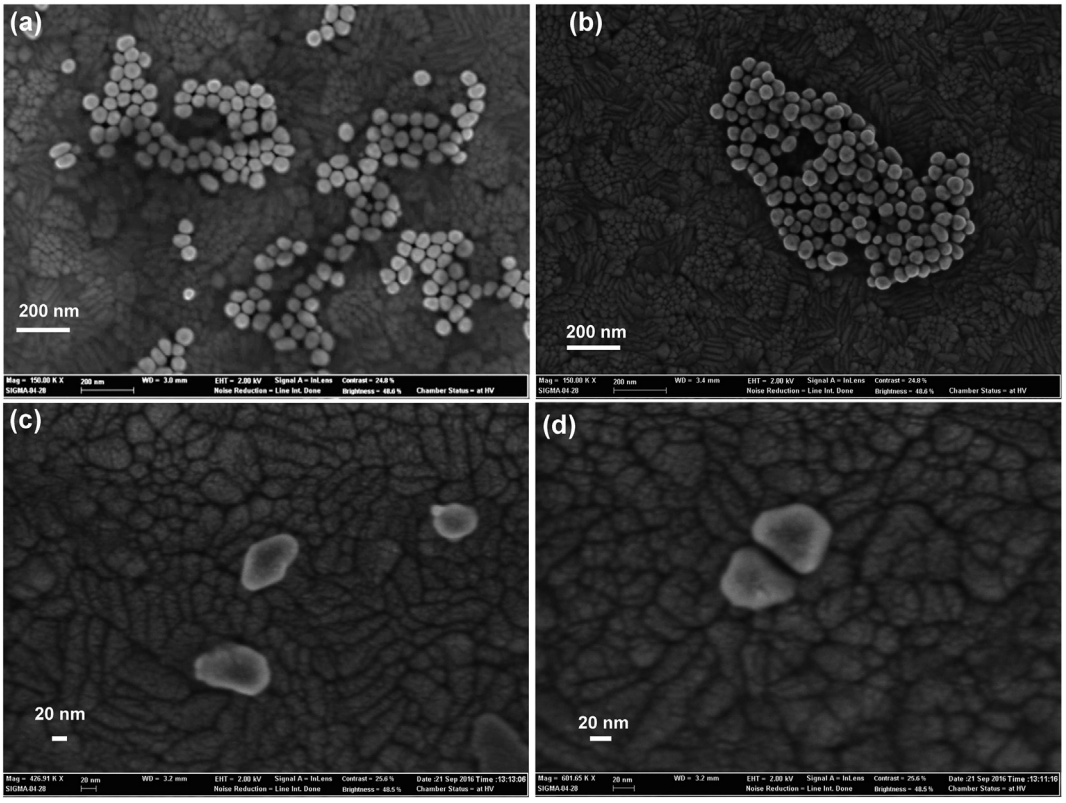

Fig. 1. SEM images of Au nanostructures at different magnification values.

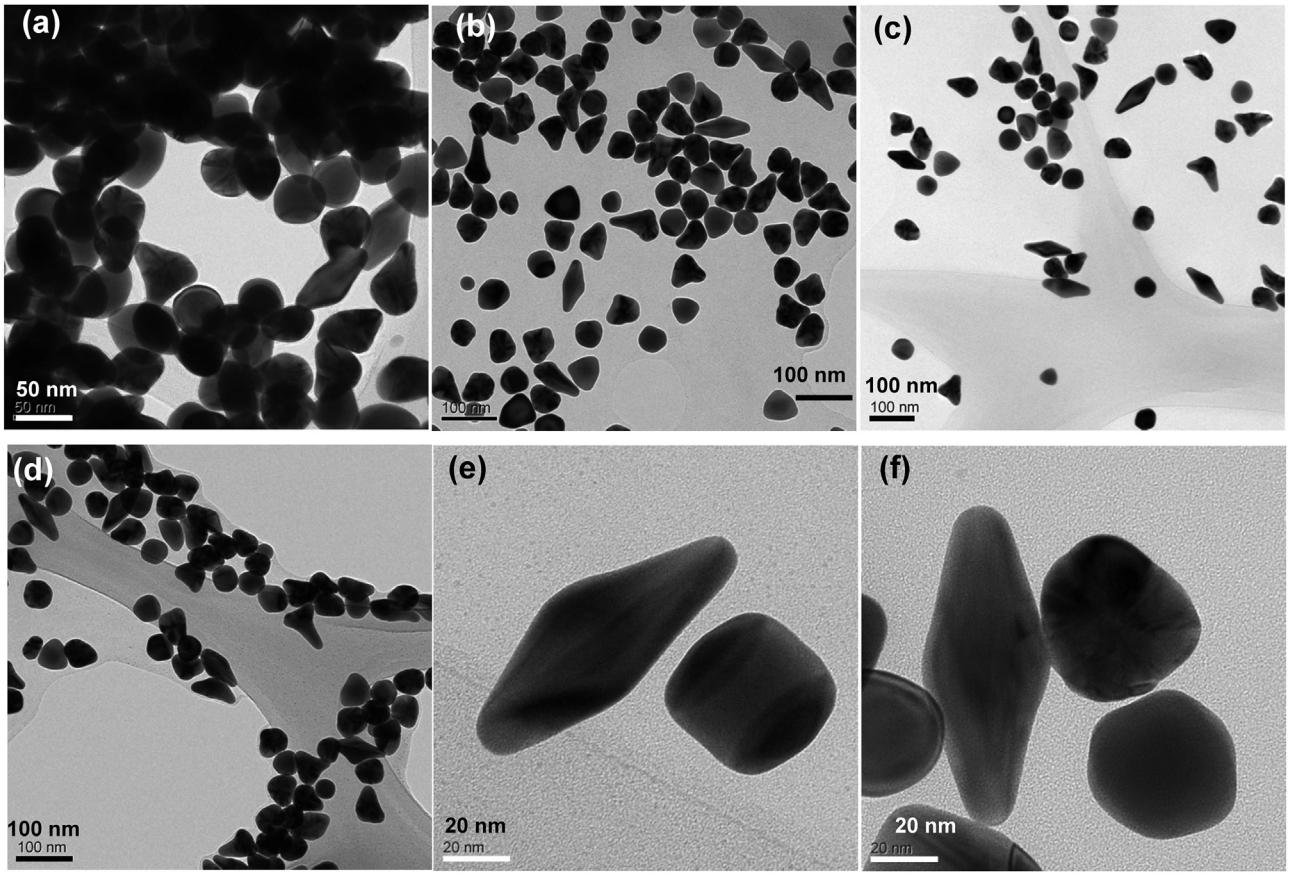

Fig. 2. TEM images of Au nanostructures at different magnification values.

Please cite this article as: W.A. El-Said, W. Alshitari and J. Choi, Controlled fabrication of gold nanobipyramids/polypyrrole for shell-isolated nanoparticle-enhanced R..., Spectrochimica Acta Part A: Molecular and Biomolecular Spectroscopy, https://doi.org/10.1016/j.saa.2019.117890

sulfate (SDS, 99%) was purchased from Fisher Scientific. Deionized water (resistivity about18.2 MΩ·cm) was used for all preparations.

2.2. Preparation of gold nanobipyramids (Au NbPs)

Au NbPs were synthesized based on the seed-mediated technique through two steps method (Scheme 1) that including the preparation of small Au seeds then allowed these seeds to grow and formation of Au NbPs in the existence of CTAB as a structure-directing agent. Typically, in the first step seeds solution was prepared as following, 0.6 mL of ice-cold $NaBH_4$ (1 mM) was mixed with a 7.75 mL (0.1 M) of aqueous solution of CTAB that contain 0.323 mM of chloroauric acid under stirring for 2 min and then the reaction mixture was kept at room temperature for 1 h to obtain the seeds solution. In the second step, a growth solution consists of a mixture of 0.1 M CTAB, a solution of 0.1 mM of chloroauric acid and 7 mL (1 M) of ascorbic acid. Finally, the seed solution was ten times diluted with deionized water (DIW) and 0.35 mL of the diluted solution was added to the growth solution and leave to grow for 4 h.

2.3. Fabrication of Au nanobipyramids/polypyrrole core/shell

Au NbPs@PPy core/shell nanostructures were synthesized based on chemical polymerization of the pyrrole monomer by using ammonium persulfate [49,50]. In the beginning, the extra CTAB was removed from the surface of the Au NbPs before preparing Au NbPs@PPy core/shell nanostructures by centrifuge the Au NbPs solution at 4000 rpm for 10 min. After removing the supernatant, the residual was redispersed in DIW. Then, 3.5 mL of the CTAB-wrapped Au NbPs were separated by using the centrifuge at a speed of 4000 rpm for 10 min, and the concentrated Au NbPs were redistributed in 2 mL a mixture of 2 mM of pyrrole and 0.25 mL of 40 mM SDS, and vortex the reaction mixture for 1 min for complete mixing. Finally, 1.5 mL of 2 mM of ammonium persulfate dissolved in 10 mM of an aqueous solution of HCl was added to

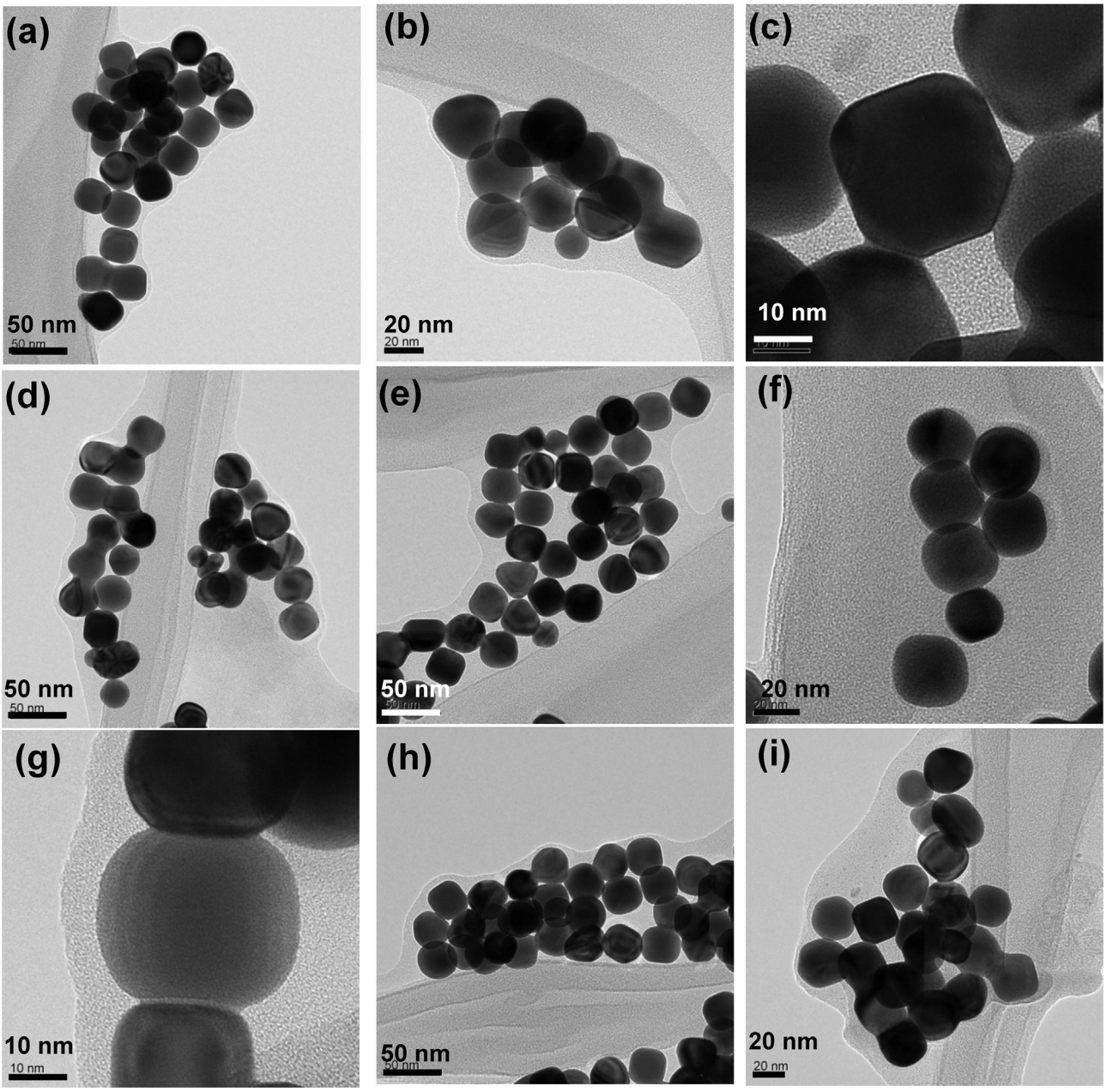

Fig. 3. TEM images of Au nanocubes at different magnification values.

Please cite this article as: W.A. El-Said, W. Alshitari and J. Choi, Controlled fabrication of gold nanobipyramids/polypyrrole for shell-isolated nanoparticle-enhanced R..., Spectrochimica Acta Part A: Molecular and Biomolecular Spectroscopy, https://doi.org/10.1016/j.saa.2019.117890

the above mixture (Au NbPs, pyrrole, and SDS) and vortexed for 10 s and kept at room temperature for 24 h for complete polymerization. The Au NbPs@PPy core/shell nanostructures were obtained by centrifuge at 6000 rpm for 10 min and redispersed in 1.5 mL of 3.6 mM SDS solution. The surface morphologies of the Au NbPs and Au NbPs@PPy were analyzed by a field-emission scanning electron microscope (FE-SEM) (Zeiss SIGMA VP-FESEM).

2.4. Fabrication of neurotransmitters sensor

At the beginning, a monolayer of the Au NbPs was formed over an ITO substrate as following, 100 μL of Au NbPs solution was added to an ITO substrate (1 cm × 1 cm) and dispersed by using spin-coated at a spin speed of 1000 rpm for 1 min, then allowed the substrate to dry under a constant drying ambient and evaporation rate [10]. Then, ten microliters of the neurotransmitters with different concentrations were drop-casted onto the Au NbPs/ITO substrate and allowed for immobilization based on self-assembly assay for 1 h under humid conditions to avoid the dryness of the samples. Finally, the modified substrates were rinsed with DIW and dried with N_2 gas and used directly for the Raman spectra measurements.

2.5. Raman measurements

The chemical composition of the prepared Au NbPs/PPy, the SERS efficiency of Au NbPs/PPy core-shell and its applications were studied by Raman spectroscopy using Raman NTEGRA spectra (NT-MDT, Russia). The resolution of the spectrometer was 200 in the XY plane nm and 500 nm along the *Z*-axis. The SERS spectra were recorded by using near-infrared laser emitting light at a 785 nm wavelength, at 50× objective with a spot size of 620 nm. The maximum scan-range, XYZ was 100 μm × 100 μm × 6 μm. Five scans of 5 s accumulation time within a range from 200 cm^{-1} to 2000 cm^{-1} were measured at different random spots and the average data was used.

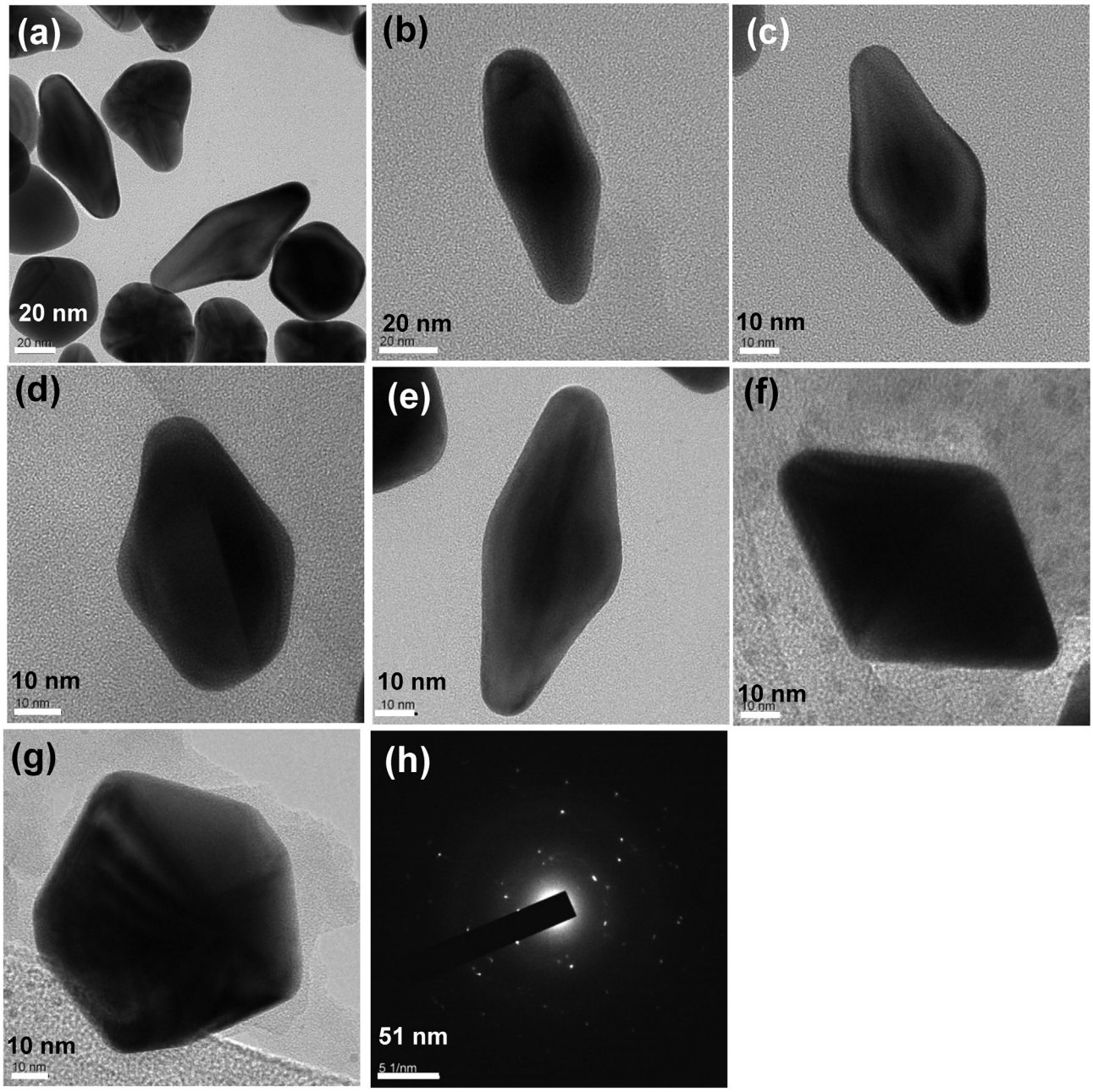

Fig. 4. (a & b) TEM images of Au NbPs, scale bar 20 nm, (c–g) TEM images of Au NbPs, scale bar 10 nm and (h) HR-TEM image of Au NbPs.

Please cite this article as: W.A. El-Said, W. Alshitari and J. Choi, Controlled fabrication of gold nanobipyramids/polypyrrole for shell-isolated nanoparticle-enhanced R..., Spectrochimica Acta Part A: Molecular and Biomolecular Spectroscopy, https://doi.org/10.1016/j.saa.2019.117890

3. Results and discussion

3.1. Control preparation of gold nanobipyramids

Here, we have fabricated Au nanostructures coated with a thin film of polypyrrole as shown in Scheme 1. Firstly, the Au nanostructures were prepared by using $NaBH_4$ as a reducing agent. The morphology of the prepared Au nanostructures was studied by using FE-SEM and HR-TEM techniques. Fig. 1 showed the SEM images of the Au nanostructures at different magnifications that illustrated the formation of two morphologies. Furthermore, TEM was used to investigate the morphology of the obtained Au nanostructures (Fig. 2), which showed the formation of a mixed two forms nanobipyramids and rounded nanocubes. This mixture of the Au nanobipyramids and rounded nanocubes was separate based on a centrifuge at different speeds since we obtained the Au nanobipyramids after centrifuged the Au nanostructures solution at 4000 rpm for 10 min; while Au rounded nanocubes were obtained after centrifuged the residual at 6000 rpm for 10 min. It is obvious that the obtained Au NbPs were stable in the solution for a long time without noticeable precipitation due to the existence of CTAB on the Au surface. However, repeating of centrifuge several times results in the CTAB dissociation from the Au NbPs that led to an irreversible aggregation of the Au nanostructures [51]; thus it isn't recommended to repeat the centrifuge process. Fig. 3 showed the TEM images of Au rounded nanocubes that illustrated the formation of highly uniform rounded nanocubes; the lengths of the edges of the rounded nanocubes were analyzed by using SPIP program by analyzed 23 particles (Fig. S1), which demonstrated that the lengths of the average edges of the nanocubes were 20 nm. Furthermore, Fig. 4 showed the TEM images of the Au NbPs. The width of the NbPs was analyzed by using SPIP as shown in Fig. S2, which demonstrated that the average width size was about 14 ± 4 nm.

3.2. Preparation of gold nanobipyramids/polypyrrole core/shell

A thin film of polypyrrole was formed as an isolated shell on Au NbPs; the morphology of the Au NbPs@PPy core/shell was investigated by using the TEM technique as shown in Fig. 5, which demonstrated the formation of ultrathin PPy film of a thickness of 1 nm. The formation of the PPy layer was resulted in changing the solution color from pink to green color as shown in Fig. S3. The presence of this polymer film could result in addition to enhancing in the Raman intensity, protect the Au nanostructures from the accumulation and increase the adsorption of the neurotransmitters onto the Au nanostructures.

3.3. UV–vis of gold nanobipyramids/polypyrrole core/shell

Fig. 6a represented the UV–vis absorption spectrum of Au NbPs@PPy, which clearly showed two absorption bands, one at λ_{max} of about 412 nm (within the visible region) that could be attributed to the transverse electronic oscillation. Furthermore, the second band was within the near-infrared region at λ_{max} of about 796 nm, which owing to the longitudinal oscillation of the conduction band electrons, which is more sensitive towards the local dielectric environment than the absorption band that results from the transverse electronic oscillation [7]. Furthermore, the formation of the PPy layer was confirmed by using the Raman technique. Fig. 6b showed the Raman spectra of five different spots, which showed the same Raman peaks with narrow variation in the peaks' intensities that indicated the homogeneous of the polymer film. Raman spectrum of the Au NbPs/PPy (Fig. 6b) showed the characteristic bands of PPy film that including band at 1055 cm^{-1} (C—H in-plane bending vibration of PPy), band at 1176 cm^{-1} (CH in-plane bending mode of quinoid and semiquinoid rings). In addition, a band at 1250 cm^{-1} (N—H in-plane deformation) and two bands at 1349 cm^{-1} (inter-ring C—C stretching) and 1502 cm^{-1} (C═N

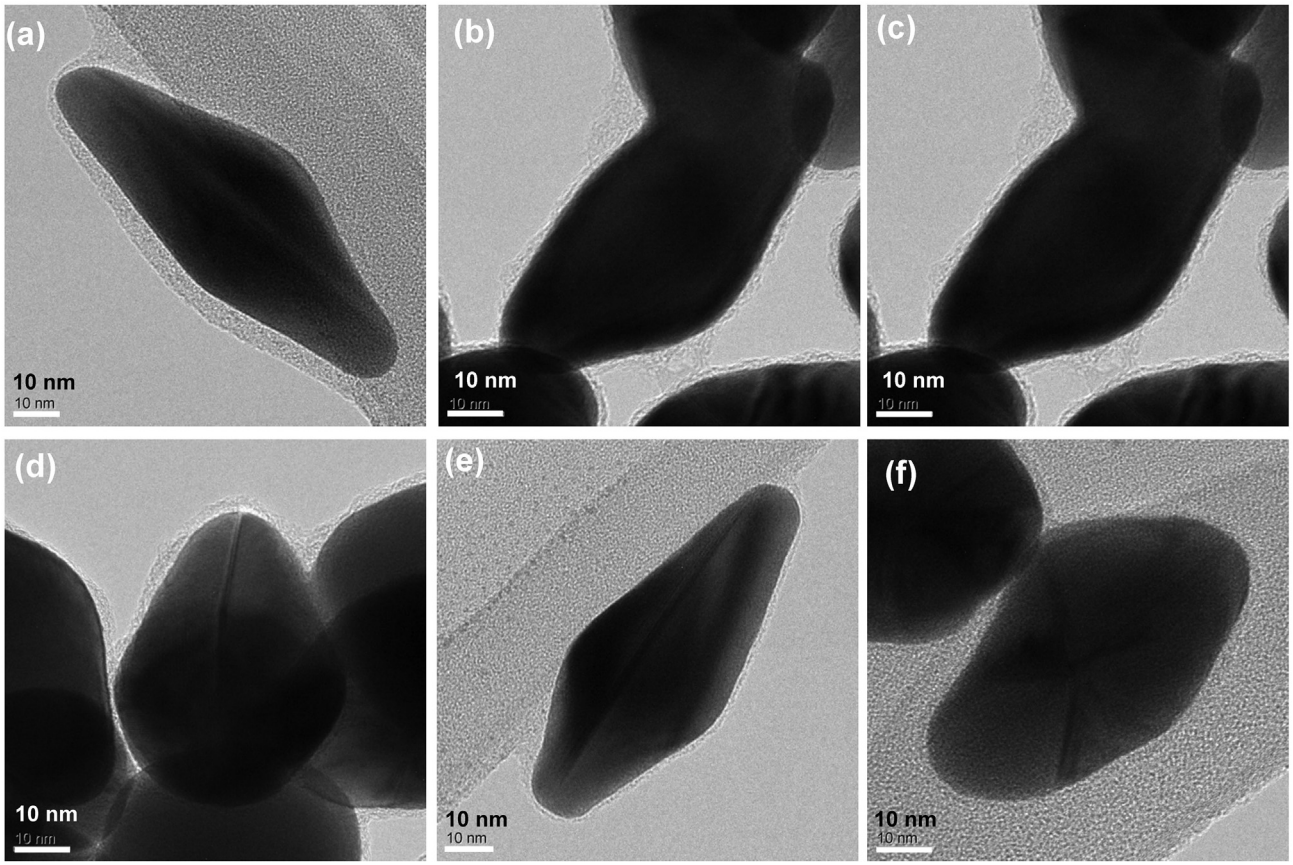

Fig. 5. TEM images of Au NbPs/PPy, scale bar 10 nm.

Please cite this article as: W.A. El-Said, W. Alshitari and J. Choi, Controlled fabrication of gold nanobipyramids/polypyrrole for shell-isolated nanoparticle-enhanced R..., Spectrochimica Acta Part A: Molecular and Biomolecular Spectroscopy, https://doi.org/10.1016/j.saa.2019.117890

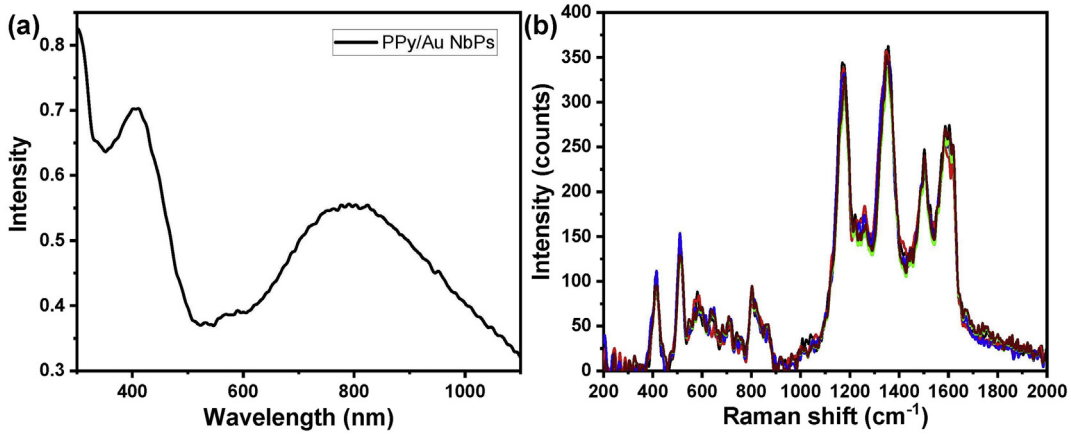

Fig. 6. (a) UV–vis. absorption spectra of Au NbPs/PPy and (b) SERS spectra of Au NbPs@PPy at different spots.

stretching for quinine diimine structure). Furthermore, there are two bands at 1592 cm^{-1} and 1613 cm^{-1} (C═C symmetry stretching). These results confirmed the formation of PPy onto the surface of the Au NbPs.

3.4. Monitoring of different neurotransmitters

Before recording the Raman spectra of different neurotransmitters, the Raman spectrum of Au NbPs/PPy (Fig. 6b) was as a blank spectrum. Ten microliters of the neurotransmitters solution (10 μM) were self-assembled on the Au NbPs/PPy and then the SERS spectra were recorded five times and the average data were represented in Fig. 7. The SERS spectrum of GABA neurotransmitters was represented in Fig. 7a, which displayed a set of Raman bands including 885 cm^{-1} that related to the C-C-N band and the strong band at 1018 cm^{-1} assigned to deformation of CH_2. Also, Raman bands at 1105 cm^{-1} (NH_2 band), 1344 cm^{-1} (CH_2 band) and a shoulder band at 1387 cm^{-1} that assigned to the stretching vibration of OCO, which indicated the immobilization of adsorbed amino acid. In addition to the Raman band at 1065 cm^{-1} that corresponding to the zwitterionic form of GABA. Fig. 7b showed the SERS spectrum of Glu that illustrated some characteristic Raman bands including Raman band at 757 cm^{-1} (COO– band), Raman band at 932 cm^{-1} that ascribed to the completely ionized form of Glu (stretching vibration of the C-COO), 1105 cm^{-1} (NH_2 band) and 1358 cm^{-1} related to the symmetrical stretching vibration of the COO– group. Fig. 8a displays the average SERS spectra of different concentrations of GABA that illustrated an increase in the Raman intensities with increasing the GABA concentration. Fig. 8b represented the

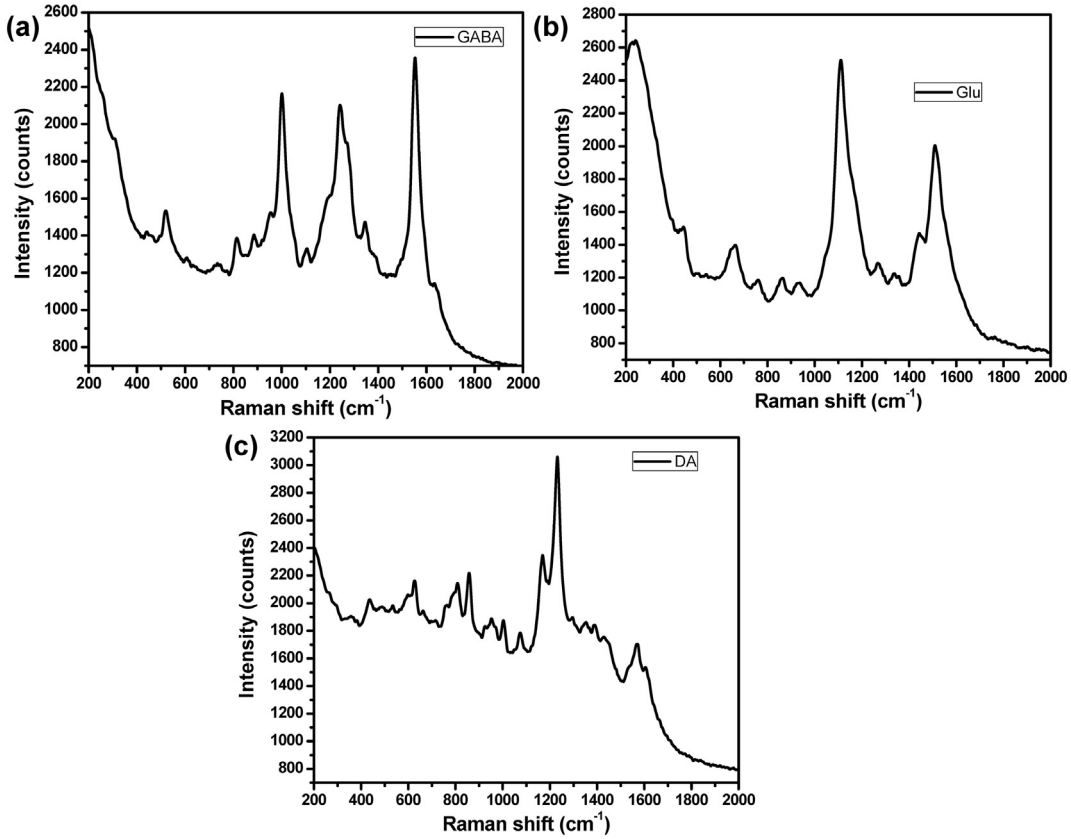

Fig. 7. Raman spectrum of (a) GABA and (b) Glu dissolved in PBS (pH, 7.4).

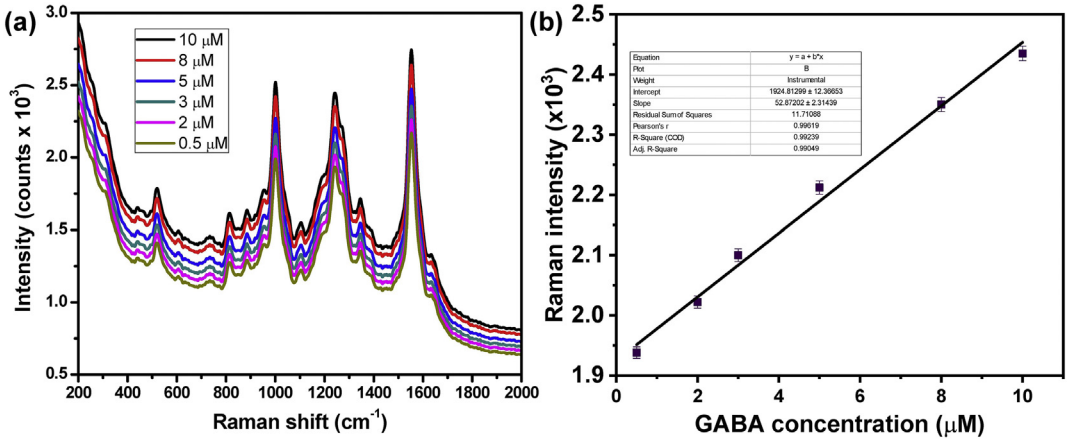

Fig. 8. (a) Average Raman spectra of different concentration of GABA, these data are the mean of five scans at different spots for each concentration and (b) relationship between the GABA concentrations and the Raman intensity of the Raman band at 1334 cm^{-1}.

relationship between the GABA concentration and the intensity of the Raman signal at 1344 cm^{-1}, which displayed a linear relationship with an R^2 of about 0.9923. The LOD of the GABA was calculated as following, (LOD = 3.3 * (STEYX/Slope of calibration curve)), and it was found equal 116 nM.

3.5. Gold nanobipyramids/polypyrrole core/shell for a neurotransmitter in real samples

The capability of the used sensor for the detection of the GABA neurotransmitter in a real sample was investigated based on monitoring a low concentration of GABA dissolved in PBS contains human serum (HS, 1%) as a represented real sample. The Raman spectrum of HS was demonstrated in Fig. 9a, which showed a set of peaks at 820, 1044, 1335, 1383, 1442, and 1614 cm^{-1} those corresponding to the starching vibration of CH_2 & CH_3 groups of lipids and proteins; also, Raman peak at 1653 cm^{-1} for Amide *I* and Lipid. Fig. 9b showed the Raman spectrum of 5 μM of GABA soluble in PBS solutions containing HS after subtracted the Raman spectrum corresponding to the HS molecules, which displayed a set of Raman bands similar to the Raman spectrum of GABA dissolved in PBS buffer with a little difference in the strength of some bands that confirmed the ability of this Au NbPs/PPy to measure GABA in human serum sample without any interference-effect.

4. Conclusions

This work reported the design and fabrication of new hybrid organic/inorganic material (Au nanobipyramids/polypyrrole) and its uses for enhancing the Raman intensity based on SHINERS. The biosensor with nanobipyramids/polypyrrole was used for the simultaneous detection of different neurotransmitters, GABA and glutamate. The high sensitivity of this biosensor based on SHINERS allowed monitoring the low concentration of GABA with a LOD of 116 nM. The proposed biosensor can be applied to detect various neurotransmitters for diagnosing neural disorders with high sensitivity.

Declaration of competing interests.

The authors declare that they have no known competing financial interests or personal relationships that could have appeared to influence the work reported in this paper.

Authors' contributions

J.W. Choi and W.A. El-Said suggest the point, synthesized the materials and measured all the required characterization techniques and participate in writing the manuscript and discuss the data. Wael Alshitari participates in discussing the results, analyzing the data and revised the manuscript finally. In addition, all authors read and approved the final manuscript.

Funding sources

Waleed El-Said was funded by the Brain Pool program funded by the Ministry of Science and ICT through the National Research Foundation of Korea (171S-4-3-1800).

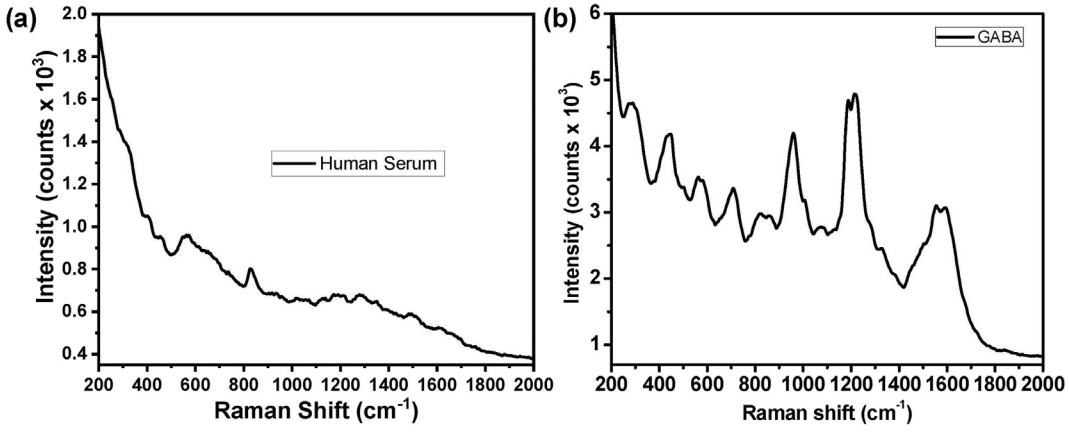

Fig. 9. Raman spectrum of GABA dissolved in human serum.

Please cite this article as: W.A. El-Said, W. Alshitari and J. Choi, Controlled fabrication of gold nanobipyramids/polypyrrole for shell-isolated nanoparticle-enhanced R..., Spectrochimica Acta Part A: Molecular and Biomolecular Spectroscopy, https://doi.org/10.1016/j.saa.2019.117890

Declaration of competing interest

The authors declare no competing financial interests.

Acknowledgments

This research was supported by the Brain Pool program funded by the Ministry of Science and ICT through the National Research Foundation of Korea (171S-4-3-1800).

Appendix A. Supplementary data

Supplementary data to this article can be found online at https://doi.org/10.1016/j.saa.2019.117890.

References

[1] K. Kneipp, M. Moskovits, H. Kneipp, Surface-Enhanced Raman Scattering: Physics and Applications, Springer-Verlag, Berlin and Heidelberg, 2006.
[2] K. Kneipp, H. Kneipp, I. Itzkan, R.R. Dasari, M.S. Feld, Surface-enhanced Raman scattering and biophysics, J. Phys. Condens. Matter 14 (2002) R597–R624.
[3] W.A. El-Said, S.U. Kim, J.-W. Choi, Monitoring in vitro neural stem cell differentiation based on surface-enhanced Raman spectroscopy using a gold nanostar array, J. Mater. Chem. C 3 (2015) 3848.
[4] W.A. El-Said, T.-H. Kim, Y.-H. Chung, J.-W. Choi, Fabrication of new single cell chip to monitor intracellular and extracellular redox state based on spectroelectrochemical method, Biomaterials 40 (2015) 80–87.
[5] J.-H. An, W.A. El-Said, C.-H. Yea, T.-H. Kim, J.-W. Choi, Surface-enhanced Raman scattering of dopamine on self-assembled gold nanoparticles, J. Nanosci. Nanotechnol. 11 (2011) 4424–4429.
[6] W.A. El-Said, T.-H. Kim, C.-H. Yea, H.C. Kim, J.-W. Choi, Fabrication of gold nanoparticle modified ITO substrate to detect β-amyloid using surface-enhanced Raman scattering, J. Nanosci. Nanotechnol. 11 (2011) 768–772.
[7] W.A. El-Said, T.-H. Kim, H.C. Kim, J.-W. Choi, Detection of effect of chemotherapeutic agents to cancer cells on gold nanoflower patterned substrate using surface enhanced Raman scattering and cyclic voltammetry, Biosens. Bioelectron. 26 (2010) 1486–1492.
[8] J.-W. Shin, J. Yoon, M. Shin, and J.-W. Choi, Electrochemical dopamine biosensor composed of silver encapsulated MoS_2 hybrid nanoparticle, Biotechnol. Bioprocess Eng., doi:https://doi.org/10.1007/s12257-018-0350-1.
[9] J.-H. Lee, E.-J. Chae, S.-J. Park, J.-W. Choi, Label-free detection of γ-aminobutyric acid based on silicon nanowire biosensor, Nano Convergence (2019) https://doi.org/10.1186/s40580-019-0184-3.
[10] W.A. El-Said, J.-W. Choi, Electrochemical biosensor consisted of conducting polymer layer ongold nanodots patterned indium tin oxide electrode for rapid and simultaneous determination of purine bases, Electrochim. Acta 123 (2014) 51–57.
[11] N.G. Bowery, T.G. Smart, GABA and glycine as neurotransmitters: a brief history, Br. J. Pharmacol. 147 (Suppl. 1) (2006) S109–S119.
[12] S. Ozawa, H. Kamiya, K. Tsuzuki, Glutamate receptors in the mammalian central nervous system, Prog. Neurobiol. 54 (1998) 581–618.
[13] J.H. Yi, A.S. Hazell, Excitotoxic mechanisms and the role of astrocytic glutamate transporters in traumatic brain injury, Neurochem. Int. 48 (2006) 394–403.
[14] D.C. Javitt, Glutamate as a therapeutic target in psychiatric disorders, Mol. Psychiatry 9 (2004) 984–997.
[15] G. Sperk, S. Furtinger, C. Schwarzer, S. Pirker, GABA and its receptors in epilepsy, Adv. Exp. Med. Biol. 548 (2004) 92–103.
[16] G. Helms, C. Ciumas, S. Kyaga, I. Savic, Increased thalamus levels of glutamate and glutamine (Glx) in patients with idiopathic generalized epilepsy, J. Neurol. Neurosurg. Psychiatry 77 (2006) 489–494.
[17] W.R.W. Martin, MR spectroscopy in neurodegenerative disease, Mol. Imaging Biol. 9 (2007) 196–203.
[18] J.M. Stone, P.D. Morrison, L.S. Pilowsky, Glutamate and dopamine dysregulation in schizophrenia - a synthesis and selective review, J Psychopharmacol (Oxf) 21 (2007) 440–452.
[19] K. Buck, P. Voehringer, B. Ferger, Rapid analysis of GABA and glutamate in microdialysis samples using high performance liquid chromatography and tandem mass spectrometry, J. Neurosci. Methods 182 (2009) 78–84.
[20] Y. Song, M. Shenwua, D.M. Dhosscheb, Y.M. Liua, A capillary liquid chromatographic-tandem mass spectrometric method for the quantification of GABA in human plasma and cerebrospinal fluid, J. Chromatogr. B 814 (2005) 295–302.
[21] B.B. Carlson, S. Behrstock, A.J. Tobin, J.D. Salamone, Brain implantations of engineered GABA-releasing cells suppress tumor in an animal model of Parkinsonism, Neuroscience 119 (4) (2003) 927–932.
[22] S. Zhang, Y. Takeda, S. Hagioka, K. Takata, H. Aoe, H. Nakatsuka, et al., Measurement of GABA and glutamate in vivo levels with high sensitivity and frequency, Brain Res. Protocol. 14 (2005) 61–66.
[23] A.J. Devall, R. Blake, N. Langman, C.G.S. Smith, D.A. Richards, K.J. Whitehead, Monolithic column-based reversed-phase liquid chromatography separation for amino acid assay in microdialysates and cerebral spinal fluid, J. Chromatogr. B 848 (2007) 323–328.
[24] W. Sheng, H.W. Hang, D.Y. Ruan, In vivo microdialysis study of the relationship between lead-induced impairment of learning and neurotransmitter changes in the hippocampus, Environ. Toxicol. Pharmacol. 20 (2005) 233–240.
[25] G. Clarke, S. O'Mahony, G. Malone, T.G. Dinan, An isocratic high-performance liquid chromatography method for the determination of GABA and glutamate in discrete regions of the rodent brain, J. Neurosci. Methods 160 (2007) 223–230.
[26] V. Sauvinet, et al., In vivo simultaneous monitoring of aminobutyric acid, glutamate, and LVAspartate using brain microdialysis and capillary electrophoresis with laser-induced fluorescence detection: analytical developments and in vitro/in vivo validations, Electrophoresis 24 (2003) 3187–3196.
[27] L. Cao, et al., Capillary electrophoresis-laser induced fluorescence detection of GABA and its analogs in human serum with solid-phase extraction and fluorescein-based probes, Anal. Methods 5 (2013) 6000–6008.
[28] R.J. Dijkstra, et al., Monitoring neurotransmitter release using surface-enhanced Raman spectroscopy, J. Neurosci. Methods 159 (2007) 43–50.
[29] N. Peica, C. Lehene, N. Leopold, S. Schlucker, W. Kiefer, Monosodium glutamate in its anhydrous and monohydrate form: differentiation by Raman spectroscopies and density functional calculations, Spectrochim. Acta A 66 (2007) 604–615.
[30] P.D. O'Neal, G.L. Cote, M. Motamedi, J. Chen, W. Lin, Feasibility study using surface-enhanced Raman spectroscopy for the quantitative detection of excitatory amino acids, J. Biomed. Opt. 8 (2003) 33–39.
[31] V. Tiwari, A. Khetani, A.M.T. Monfared, B. Smith, H. Anis, Detection of Amino Acid Neurotransmitters by Surface Enhanced, Presented at Reporters, Markers, Dyes, Nanoparticles, Molecular Probes Biomedical Applications IV, San Francisco, CA, USA, 2012 (Art. ID. 82330Q).
[32] R.T. Kenedy, C.J. Watson, W.E. Haskins, D.H. Powell, R.E. Strecker, In vivo neurochemical monitoring by microdialysis and capillary separations, Current Opinion Chem. Biol. 6 (2002) 659–665.
[33] J.F. Li, Y.F. Huang, Y. Ding, Z.L. Yang, S.B. Li, X.S. Zhou, F.R. Fan, W. Zhang, Z.Y. Zhou, D.Y. Wu, B. Ren, Z.L. Wang, Z.Q. Tian, Shell-isolated nanoparticle-enhanced Raman spectroscopy, Nature 464 (2010) 392–395.
[34] J.F. Li, J.R. Anema, T. Wandlowski, Z.Q. Tian, Dielectric shell isolated and graphene shell isolated nanoparticle enhanced Raman spectroscopies and their applications, Chem. Soc. Rev. 44 (2015) 8399–8409.
[35] Y.-F. Huang, C.-Y. Li, I. Broadwell, J.-F. Li, D.-Y. Wu, B. Ren, Z.-Q. Tian, Shell-isolated nanoparticle-enhanced Raman spectroscopy of pyridine on smooth silver electrodes, Electrochim. Acta 56 (2011) 10652–10657.
[36] J.R. Anema, J.-F. Li, Z.-L. Yang, B. Ren, Z.-Q. Tian, Shell-isolated nanoparticle-enhanced Raman spectroscopy: expanding the versatility of surface-enhanced, Annu. Rev. Anal. Chem. 4 (2011) 129–150.
[37] T.A. Galloway, L.J. Hardwick, Utilizing in situ electrochemical SHINERS for oxygen reduction reaction studies in aprotic electrolytes, J. Phys. Chem. Lett. 7 (2016) 2119–2124.
[38] A. Zdaniauskienė, T. Charkova, I. Matulaitienė, O. Eicher-Lorka, A. Matijoška, M. Skapas, A. Selskis, G. Niaura, Electrochemical shell-isolated nanoparticle-enhanced Raman spectroscopy: bonding, structure, and ion-pairing of the positive charge bearing pyridinium ring terminated monolayer at smooth gold electrode, J. Phys. Chem. C 122 (2018) 1234–1242.
[39] D.P. Butcher Jr., S.P. Boulos, C.J. Murphy, R.C. Ambrosio, A.A. Gewirth, Face-dependent shell-isolated nanoparticle enhanced Raman spectroscopy of 2,2′-Bipyridine on Au(100) and Au(111), J. Phys. Chem. C 116 (2012) 5128–5140.
[40] J.F. Li, X.D. Tian, S.B. Li, J.R. Anema, Z.L. Yang, Y. Ding, Y.F. Wu, Y.M. Zeng, Q.Z. Chen, B. Ren, Z.L. Wang, Z.Q. Tian, Surface analysis using shell-isolated nanoparticle-enhanced Raman spectroscopy, Nat. Protoc. 8 (2013) 52–65.
[41] C. Zheng, L. Liang, S. Xu, H. Zhang, C. Hu, L. Bi, Z. Fan, B. Han, W. Xu, The use of Au@SiO_2 shell-isolated nanoparticle-enhanced Raman spectroscopy for human breast cancer detection, Anal. Bioanal. Chem. 406 (2014) 5425–5432.
[42] C.-Y. Li, J.-C. Dong, X. Jin, S. Chen, R. Panneerselvam, A.V. Rudnev, Z.-L. Yang, J.-F. Li, T. Wandlowski, Z.-Q. Tian, In situ monitoring of electrooxidation processes at gold single crystal surfaces using shell-isolated nanoparticle-enhanced Raman spectroscopy, J. Am. Chem. Soc. 137 (2015) 7648–7651.
[43] S. Guan, O. Donovan-Sheppard, C. Reece, D.J. Willock, A.J. Wain, G.A. Attard, Structure sensitivity in catalytic hydrogenation at platinum surfaces measured by shell-isolated nanoparticle enhanced Raman spectroscopy (SHINERS), ACS Catal. 6 (2016) 1822–1832.
[44] B.-Y. Wen, X. Jin, Y. Li, Y.-H. Wang, C.-Y. Li, M.-M. Liang, R. Panneerselvam, Q.-C. Xu, D.-Y. Wu, Z.-L. Yang, J.-F. Li, Z.-Q. Tian, Shell-isolated nanoparticle-enhanced Raman spectroscopy study of the adsorption behaviour of DNA bases on Au(111) electrode surfaces, Analyst 141 (2016) 3731–3736.
[45] T. Hartman, C.S. Wondergem, B.M. Weckhuysen, Practical guidelines for shell-isolated nanoparticle-enhanced Raman spectroscopy of heterogeneous catalysts, ChemPhysChem 19 (2018) 2461–2467.
[46] J.-S. Li, S.-L. Li, Y.-J. Tang, K. Li, L. Zhou, N. Kong, Y.-Q. Lan, J.-C. Bao, Z.-H. Dai, Heteroatoms ternary-doped porous carbons derived from MOFs as metal-free electrocatalysts for oxygen reduction reaction, Sci. Rep., 4, 5130, doi: https://doi.org/10.1038/srep05130.
[47] X. Wang, Y. Shen, A. Xie, S. Chen, One-step synthesis of Ag@PANI nanocomposites and their application to detection of mercury, Mater. Chem. Phys. 140 (2013) 487–492.
[48] R.A. Álvarez-Puebla, R. Contreras-Cáceres, I. Pastoriza-Santos, J. Pérez-Juste, L.M. Liz-Marzán, Au@pNIPAM colloids as molecular traps for surface-enhanced, spectroscopic, ultra-sensitive analysis, Angew. Chem. Int. Ed. 48 (2009) 138–143.
[49] N.N. Jiang, L. Shao, J.F. Wang, (Gold Nanorod Core)/(Polyaniline Shell) Plasmonic switches with large plasmon shifts and modulation depths, Adv. Mater. 26 (2014) 3282–3289.

Please cite this article as: W.A. El-Said, W. Alshitari and J. Choi, Controlled fabrication of gold nanobipyramids/polypyrrole for shell-isolated nanoparticle-enhanced R..., Spectrochimica Acta Part A: Molecular and Biomolecular Spectroscopy, https://doi.org/10.1016/j.saa.2019.117890

[50] S. Xing, L.H. Tan, M. Yang, M. Pan, Y. Lv, Q. Tang, Y. Yang, H. Chen, Highly controlled core/shell structures: tunable conductive polymer shells on gold nanoparticles and nanochains. J. Mater. Chem. 19 (2009) 3286–3291.

[51] A.J. Schmidt, J.D. Alper, M. Chiesa, G. Chen, S.K. Das, K. Hamad-Schifferli, Probing the gold nanorod−ligand−solvent interface by plasmonic absorption and thermal decay, J. Phys. Chem. C 112 (2008) 13320–13323.

Please cite this article as: W.A. El-Said, W. Alshitari and J. Choi, Controlled fabrication of gold nanobipyramids/polypyrrole for shell-isolated nanoparticle-enhanced R..., Spectrochimica Acta Part A: Molecular and Biomolecular Spectroscopy, https://doi.org/10.1016/j.saa.2019.117890